

# Exploring Potential Gains of Mobile Sector-Coupling Energy Systems in Heavily Constrained Networks

Mahdi Habibi , Vahid Vahidinasab , Senior Member, IEEE,  
Behnam Mohammadi-Ivatloo , Senior Member, IEEE, Jamshid Aghaei , Senior Member, IEEE,  
and Phil Taylor, Senior Member, IEEE

**Abstract**—The coincidence of high levels of variable, non-dispatchable generation from renewable energy sources (RESs) and congested electricity networks imposes significant constraint payments (CP) on electricity system operators (ESOs) which ultimately is charged to the customers. This paper is inspired by this challenge and proposes an integrated electricity, gas, and transportation energy system taking advantage of power-to-gas (P2G) facilities and electricity/gas storage devices to enhance operational efficiency. It proposes mobile gas storage systems (MGSs) that can store and carry liquid hydrogen or liquefied natural gas (LNG) to the load points or remote locations without access to the gas network. So, the green energy of RESs in the form of gases can be injected, transported, and reutilized in the natural gas network or stored in MGS facilities. Besides, the mobile electricity storage system (MES) can directly store the redundant electricity produced by RESs, and the railway transportation system carries both the MESs and MGSs to the load point of electrical and gas systems. The proposed model reflects CP to wind in the marketing phase and considers incentives for the hydrogen-burning generators. Also, a stochastic platform is employed to capture the inherent uncertainties in the predicted values of the load and RESs' generation. The model is formulated as a mixed-integer second-order cone programming problem and tested on an IEEE 118-bus system integrated with a 14-node gas network and a railway system. The result shows that employing the multi-vector energy system (MVES) elements reduces the total operational cost by 47%, and the CP to wind is reduced by 99.8% by absorbing almost the whole green energy of wind farms while relieving congestion in the electrical grid.

**Index Terms**—Integrated electricity, gas, and transportation systems, multi-vector energy systems, power-to-gas, wind energy, constraint payment, stochastic unit commitment, SOCP, uncertainty.

## NOMENCLATURE

### Indices and sets

$b, m, i/j$	Indices of electric buses, gas nodes, and railway.
$k, \tilde{k}$	Indices of MESs and MGSs.
$t/\tau, ts, s$	Indices of time, time span, and scenarios.
$g, w, x$	Indices of generators, wind farms, and P2Gs.
$y, c, p$	Indices of gas wells, compressors, and pipelines.
$H_2, CH_4$	Indices of label for hydrogen and methane.
$EN, GN, Sup$	Indices of labels for electrical/gas network and gas wells.
Ch, Dis	Indices of labels for charging and discharging.
min, max	Indices of label for minimum/maximum.
$\vartheta, \tilde{\vartheta}$	Sets of charging stations for $CH_4/H_2$ .
$\chi, \tilde{\chi}$	Sets of P2Gs generating $CH_4/H_2$ .
$\Phi, \tilde{\Phi}$	Sets of MGSs contain LNG and LH2.
$\beta, \tilde{\beta}$	Sets of gas-fired/conventional generators.
$F(p), R(p)$	Sets of inlet/outlet nodes of pipelines.
$\kappa, \Upsilon, \psi, \phi$	Sets of generation units, stations, and P2Gs connected to $b$ .
$\aleph$	Set of pipelines with installed compressor units.
$\sigma, \Theta, (\frac{\Delta}{\Lambda}), (\frac{\Xi}{\Omega})$	Sets of wells, P2Gs, stations, and G2Ps connected to $m$ .

### Parameters

$Z_1^{CH_4/H_2}, Z_2$	Energy conversion coefficients of P2Gs and G2P.
$\eta_x^{P2G, H_2/CH_4}$	Efficiency of P2G units in production of $H_2$ and $CH_4$ .
$\eta_{k/\tilde{k}, Ch/Dis}^{MES/MGS}$	Efficiency of MESs/MGSs in charging/discharging.
$T_{on}^{\min}, T_{off}^{\min}$	Minimum up/down-time of generators, (h).
$Ru_g, Rd_g$	Ramp rate limits of generators, (MW/h).
$RS_g, RD_g$	Start-up/shut-down ramp limits of generators, (MW/h).
$P_{w,t,s}^{\max}$	Maximum available wind energy in scenario $s$ , (MW).

Manuscript received 27 October 2021; revised 29 March 2022 and 13 May 2022; accepted 5 June 2022. Date of publication 13 June 2022; date of current version 20 September 2022. This work was supported by the Engineering and Physical Sciences Research Council (EPSRC) through the Supergen Energy Networks Hub 2018 under Grant no. EP/S00078X/2. Paper no. TSTE-01092-2021. (Corresponding author: Vahid Vahidinasab.)

Mahdi Habibi is with the Faculty of Electrical Engineering, Shahid Beheshti University, Tehran 1983969411, Iran (e-mail: m\_habibi@sbu.ac.ir).

Vahid Vahidinasab is with the Department of Engineering, School of Science and Technology, Nottingham Trent University, NG11 8NS Nottingham, U.K. (e-mail: vahid.vahidinasab@ntu.ac.uk).

Behnam Mohammadi-Ivatloo is with the Faculty of Electrical and Computer Engineering, University of Tabriz, Tabriz 56617, Iran, and also with the Information Technologies Application and Research Center, Istanbul Ticaret University, Istanbul, Turkey (e-mail: mohammadi@iee.org).

Jamshid Aghaei is with the Department of Electrical Engineering, School of Energy Systems, Lappeenranta-Lahti University of Technology, 53850 Lappeenranta, Finland (e-mail: aghaei@sutech.ac.ir).

Phil Taylor is with the School of Computer Science, Electrical and Electronic Engineering, and Engineering Maths, University of Bristol, BS8 1QU Bristol, U.K. (e-mail: pvc-research@bristol.ac.uk).

Color versions of one or more figures in this article are available at <https://doi.org/10.1109/TSTE.2022.3182871>.

Digital Object Identifier 10.1109/TSTE.2022.3182871

$A_{i,j}$	Incidence matrix of arcs between stations $i$ and $j$ .
$T(t)$	Incidence matrix of time steps in time span $ts$ .
$B_b^l$	Incidence matrix of lines connected to bus $b$ .
$Y_m^p$	Incidence matrix of pipelines connected to node $m$ .
$PD_{b,t}^s$	Active electrical demand in scenario $s$ , (MW).
$\rho^{GN}$	Gas price in the gas system, (\$/KCF).
$\eta_g^{CH_4/H_2}$	Efficiency of gas-fired generators.
$GD_{m,t}^{Fxd}$	Gas fixed demand of the gas system, (KCF).
$C_p$	Flow constant of pipelines, (KCF/Psig).
$C_{i,j}^{k/k}$	Cost of swapping system, (\$).
$\Omega_t^s, \Delta t$	Probability of scenarios/ length of time step, (h)
$M_1, M_2$	Coefficients used for big-M linearization method.
$CR_c^{Cmp}$	Ratio of inlet to outlet pressure of compressors.
$X(l), S$	Reactance of lines, (p.u.) and base power (MVA).
$\mu^{CP}, \mu^{H_2}$	Penalty of CP for wind and zero-carbon incentive, (\$).

#### Functions and variables

$u_{i,j}^{k,ts}$	Status of arc $ij$ of MESs/MGSs at time span $ts$ .
$\bar{u}_{k,t,i}^{MES,Ch/Dis}$	Status of MESs/MGSs in charging/discharging modes.
$p/G_{x,t,s}^{P2G}$	P2Gs' elec. consumption/gas production, (MW/KCF).
$e_{k,t,s}^{MES}$	Stored energy of MESs, (MWh).
$p/G_{k,i,t,s}^{MES,Ch/Dis}$	charging/discharging of MESs/MGSs, (MW/KCF).
$G_{k,t,s}^{MGS}$	Amount of stored gas by MGSs, (KCF).
$of_{t,s}^{EN/GN}$	Objective of electrical and gas systems, (\$).
$f(\cdot)$	Cost functions in linear form.
$I_g^t, st_g^t, sd_g^t$	Binary status of online/start-up/shut-down generators.
$p_g^s/w,t$	Electrical production of generators/wind farms, (MW).
$pc_{w,t}^s$	Wind power curtailment, (MW).
$p_{l,t}^s, \delta_{b,t}^s$	Power flow of lines, (MW)/ Voltage angle, (rad).
$G_{y,t,s}^{Sup}$	Natural gas supplied by gas wells, (KCF).
$G_{g,t,s}^{CH_4/H_2}$	Gas consumption of generators, (KCF).
$GF_{p,t}^s$	Gas flow of pipelines, (KCF).
$\pi_m^{t,s}, \Gamma_{1/2}^{p,t,s}$	Nodal gas pressure and square of it, (Psig/Psig <sup>2</sup> ).
$\lambda_{p,t}^s$	Auxiliary variable of gas pressures in SOCP model.
$h_{p,t,s}^{+/-}$	Binary variables indicating the gas flow direction.
$GF_{p,t}^{+/-}$	Gas flow in positive/negative directions, (KCF).
$G_{p,t}^s$	Absolute value of gas flow, (KCF).

## I. INTRODUCTION

**W**IND is a critical source of renewable energy around the world. According to a report by the international energy agency (IEA), annual capacity addition of over 340 GW is needed to reach 8265 GW based on the net-zero emissions scenario by the 2050 roadmap [1]. As another example, the ‘‘Ten Point Plan’’ announced by the U.K. in November 2020 [2], will lay the foundations for a green industrial revolution and specifically for increasing offshore wind farms (40 GW by 2030, which quadruple U.K. offshore wind capacity to generate more than all U.K. homes use today) and low-carbon hydrogen (5 GW production capacity by 2030) integration to the energy sector (i.e., industry, transport, power, and homes) [2]. While many countries considered directed incentives for developing renewable generation as the primary decarbonisation program, ensuring the security of supply remains the major challenge for electricity system operators (ESOs).

### A. Motivation and Aims

The aforementioned challenge of security of supply is particularly of importance when generation variability is accompanied by congestion of tie-lines in the power grid. This often results in a constraint on the output of renewable energy resources (RESs). Reference [3] studied the impact of domination of variable renewable energy generation in future power systems on the electricity price, while the power grid constraints are considered in a normal situation. In this regard, the need for constraint payments (CP) to be made to RES generations creates a significant cost for ESOs. For example, based on a report by the renewable energy foundation, over the period of 2010 to 2020, U.K. wind farms have received approximately £650 m as CP for curtailment of 8.7 TWh of electricity due to the network limits [4]. It is obvious that all of these additional costs will eventually be recovered from end-users. Maintaining the balance in the decarbonisation programs, security of supply, and affordability is a challenge that makes up the energy trilemma.

This paper aims to propose a whole energy systems approach to cope with this challenge and pave the way for the increasing wind power capacity. The proposed model will assess the value of mobile sector-coupling systems in an integrated electricity, gas, and transportation system and has a dual usage, as it can also be used by policy-makers in exploring the questions regarding energy systems integration.

### B. Literature Survey

1) *Low-Carbon Energy System*: Due to the proliferation of greenhouse gas emissions produced by conventional generators, environmental aspects and decarbonisation attract much more attention in recent studies. A promising option for decarbonizing the energy system is presented by green hydrogen [5]. Transition steps to reach a zero-carbon energy system are described in [6], and [7] presented the challenges and drivers faced by communities in Europe and the USA toward this goal. The low-carbon micro integrated electrical, gas, and heat systems in

the presence of high penetration of RESs, power-to-gas (P2G) facilities, and combined heat and power (CHPs) are considered in [8]. In transition toward a zero-carbon energy society, a %100 renewable energy system is planned by the year 2050 [6]. However, the existing electrical power transmission capacity may limit the full utilization of RESs. Therefore, congestion of power lines will suppress the excess energy production of RES. The P2G system, which is a so-called permanent P2G storage facility [9], is a technology that converts electricity into hydrogen or methane. In this regard, references [10, 11] used P2Gs and natural gas networks to absorb excess RESs' generation and to bypass the constrained electrical system. Also, [12] studied the application of novel security management for the injection of P2Gs' generated green hydrogen into the existing natural gas system. That study captured the uncertainty of RESs using a robust optimization platform. References [13], [14] considered P2Gs and hydrogen storage devices, where the extra RES energy is stored in gas storage systems.

2) *Financial Aspects*: Due to the high utilization charges and investment, P2G facilities are not economically effective when operating individually [9]. Also, double energy conversion in P2G facilities makes it less efficient. Authors of [15] studied the environmental and economic advantages of power-to-methane and power-to-hydrogen variants of P2G facilities. References [16], [17] used P2Gs to convert and store inexpensive/wasted energy to natural gas for appropriate applications. Also, P2G technology provides an option to reduce the dependency on buying natural gas from gas wells for supplying gas loads [9]. The equilibrium constraints of a profit-driven bi-level optimization with power-to-hydrogen and methane technologies are described in [18] to support the high penetration of renewable energy resources. The evaluation of financial risks for the energy and regulation markets in the presence of P2Gs and RESs is conducted in [19]. A model for real-time operation of P2Gs for relieving the distribution grid's congestion, thereby achieving additional revenues for P2Gs, is presented in [20]. The application of multi-energy carriers can increase flexibility and efficiency in a low-carbon energy system [14], [21]. The direct injection of hydrogen into the existing natural gas network can cause problems such as reduced delivery capacity and crack expansion of pipelines, and [22] suggested using hydrogen produced by P2Gs for specific users (e.g., combustion generators) that can accelerate the decarbonization. The deployment of operational reserves, regulation products, and other flexibility services provides new means to earn additional revenue and reduce the payback period of investments [23]. Reference [9] employed unlocked regulation services by P2G technologies to absorb the RESs' fluctuations. In [24], P2Gs and redundant line-pack of the gas network are used as new flexibility metrics. The application of P2Gs to reduce wind power curtailments and CP is investigated in [25], in which the gas network is employed to bypass a heavily-constrained power grid.

3) *Implementation*: The formulation of gas networks in steady-state is nonlinear [26], and the consideration of the actual model will complicate the integrated multi-energy operational planning. In this way, studies prefer to use the convex or linearized representation of the model. Reference [27] considered

a comprehensive linearized gas network based on piecewise formulation that includes pipelines, valves, and compressors. In [28], a linearized transient gas flow formulation reflects the dynamic behavior of the gas system. Reference [29] considered an alternating direction method of multipliers (ADMM) approach to address the complexity of the model and the limitation on exchanging private data, and iterative ADMM with second-order cone programming (SOCP) optimization is used in [30].

4) *Transportation as Energy Carrier*: The transportation system can affect power system operation due to the charging/discharging of electric and hybrid electric vehicles (EVs). Reference [5] considered power, heating, and transportation (scheduling of EVs) sectors to maximize the efficiency of the operation and the investment based on the carbon target of the GB 2050 energy system. Also, the usage of hydrogen fueling stations for the electrical and transportation sectors is investigated in [31]. However, the gas network is ignored, and local usage of hydrogen fueling stations can intensify electrical system congestion, especially at peak load hours. Recently, the usage of storage devices in swapping-charging using transportation systems is introduced as an energy carrier [32]–[38]. Reference [32] used the branch-and-bound and genetic algorithms to schedule the transportation of fully charged batteries and logistics at the distribution system level between cities. The optimal management of charging stations, depleted batteries, and well-charged batteries tries to maximize the revenue in [33]. A time-space model of the railway system is used in [34] to describe a robust-stochastic platform for scheduling the mobile electricity storage systems (MESs) in the presence of wind and load uncertainties. The impact of the battery swapping-charging system on ambient air quality and human health conditions is investigated by [35], employing a UC problem. The MESs are used in a restoration scheme for distribution systems and disaster areas in post-disaster in [36], [38]. The stochastic scheduling of integrated power and transportation systems considering emergency outages of electrical and railway systems' components is analyzed in [37]. Reference [39] used battery-based MESs to relieve grid congestion for delivering RESs' generations, including those located in remote locations (offshore).

### C. Research Gap

A taxonomy of existing papers and the novel aspects of this paper compared to the previous studies are presented in Table I. Based on the published works in this area, the impact of multi-vector energy systems (MVES) is not evaluated as the provider of constraint management services in heavily constrained networks. Although some investigations have been conducted on the P2G application as a flexibility provider to address the stochastic behavior of RESs in the normal operating of the energy system in [17], [19], [25], [26], [29], no research proposes the idea of regional constraint management services by using a holistic approach with the following features. These features consist of green hydrogen utilization for a transition toward the zero-carbon energy system that considers the potential of integrated gas, electricity, and railway systems to cope with

TABLE I  
COMPARISON OF THE MODEL PRESENTED BY THIS PAPER WITH THE LITERATURE

Reference	Scheduling of			Storage		Zero-Carbon Elements					Uncertainty			Model		
	EN	GN	Train	Elec.	Gas	RESSs	H2	P2Gs	MESs	MGSs	CP	Load	RES	Model	Horizon (PF)	Formulation
[16] / [8]	✓	✓	-	✓	✓	✓	-	✓	-	-	-	✓/-	✓/-	Stochastic/-	Day-ahead (OPF)	MINLP
[9], [29] / [19]	✓	✓	-	✓	✓	✓	-	✓	-	-	-	-/✓	-/✓	Stochastic/Robust	Day-ahead (UC/OPF)	MILP
[12]	✓	✓	-	-	-	✓	-	✓	-	-	-	-	✓	Robust	Day-ahead (OPF)	MILP
[13], [15] / [18]	✓	✓	-	✓	✓	✓	-	✓	-	-	-	-	-	-	Day-ahead (ED/OPF)	NLP
[20]	✓	✓	-	✓	✓	✓	-	✓	-	-	-	-	-	-	Real-time (OPF)	NLP
[21], [26]	✓	✓	-	✓	✓	✓	-	✓	-	-	-	-	-	-	Day-ahead (ED/OPF)	NLP
[22]	✓	✓	-	✓	✓	✓	-	✓	-	-	-	-	-	-	Long-term (ED)	NLP
[23]	✓	✓	-	✓	✓	✓	-	✓	-	-	-	-	-	Stochastic	Day-ahead (OPF)	MILP
[25]	✓	✓	-	✓	✓	✓	-	✓	-	-	✓	-	-	-	Day-ahead (UC)	MILP
[28]	✓	✓	-	-	-	✓	-	✓	-	-	-	-	✓	Stochastic	Day-ahead (OPF)	MILP
[30]	✓	✓	-	-	-	✓	-	✓	-	-	-	-	-	-	Day-ahead (OPF)	SOCP
[31]	-	-	-	✓	✓	✓	-	✓	-	-	-	-	-	-	Long-term (OPF)	NLP
[32]	✓	-	✓	✓	✓	✓	-	✓	-	-	-	-	-	-	Long-term (OPF)	MILP
[33]	✓	-	-	✓	-	✓	-	✓	-	-	-	-	-	Robust	Day-ahead (UC)	MILP
[34], [37] / [38]	✓	-	✓	-	-	✓	-	✓	-	-	-	✓/-	✓/-	Stochastic/-	Day-ahead (UC)	MILP
[40]	✓	✓	-	-	-	✓	-	✓	-	-	-	-	-	-	Day-ahead (OPF)	SOCP
This paper	✓	✓	✓	✓	✓	✓	✓	✓	✓	✓	✓	✓	✓	Stochastic	Day-ahead (UC)	MISOCP

uncertainties and the electricity network congestion to enhance the operational efficiency by decreasing the CP to the curtailed renewable production.

#### D. Contributions

In this paper, by the integration of electric power systems with natural gas and railway transportation infrastructures, a promising solution will be proposed to attain a balanced appearance in the energy trilemma, handling the variable RESs' output, and enhancing the flexibility of the coupled energy systems by deploying the regional constraint management services. When there is a coincidence between increases in wind generation and congestion of the tie-lines, our proposal is to use the following holistic vector-bridging system solutions to cope with the energy trilemma:

- A holistic approach to energy by coupling and integration of renewable, electricity, gas, and transport sectors;
- To use the P2G technologies not only as a coupling element between the gas and electricity, but also a facilitator for integration of those vectors with renewable and transportation sectors that convert redundant wind generation in heavily congested areas into the methane/hydrogen and then injecting methane into the natural gas grid or using them for charging the liquid hydrogen (LH2) or liquefied natural gas (LNG) tanks for transportation by railways system;
- To incentivise the usage of green hydrogen and supply remote gas generators by LH2 or LNG tanks transported through the railway system;
- To evaluate the impact of uncertainties due to the variable output of wind farms and load forecasting errors on the proposed framework using a stochastic formulation and study various configurations of elements and sensitivity evaluations from different aspects.

#### E. Organization of This Paper

The rest of the paper is organized as follows. Section II presents the model of MVESs, and the stochastic scheduling

of the proposed MVES coordinated with the constraint management is described in Section III. The simulation results are discussed in Section IV, and Section V concludes this paper.

## II. MODEL OF MVES

The concept and the formulation of MVES are presented in this section. The formulation includes the swapping system and the elements of MVESs and complementary energy carriers.

### A. The MVES Concept

This paper offers three options illustrated in Fig. 1(a), which take advantage of multi-type energy carriers for harvesting unserved generation of wind farms. The first option applies the gas network as a supplemental energy carrier. The P2G units enable the operators to absorb the unserved wind generation (due to the congestion in power lines or the variations in the output of wind farms), convert it into methane, inject it into the gas network, and transfer it to the areas with high demands. The produced gas can supply the non-electric gas demands or combustion generators to generate electricity. The second and third options employ the transportation system as a supplementary energy carrier. As the second option, the redundant energy of wind can be used to charge MESs and transported to the load point using the railway system. The MESs can deliver energy and plays the role of energy carrier. As the third option, the green energy of wind is converted to gas, and mobile gas storage systems (MGSs) charge liquid hydrogen (LH2) or liquefied natural gas (LNG) tanks with hydrogen or methane generated by P2G units. The railway system carries LH2 and LNG tanks to the destination areas to supply the remote gas-fired generators, also called gas-to-power (G2P) elements, with no access to the gas network. The delivered amount of energy is used for supplying gas demands or inverted to the electricity by the methane-fired or hydrogen-burning generators.

### B. The Swapping System of MVES

A time-space network (TSN) technique is applied to simulate the swapping schedule of storage devices, including MESs and MGSs, through the railway transportation system. A schematic

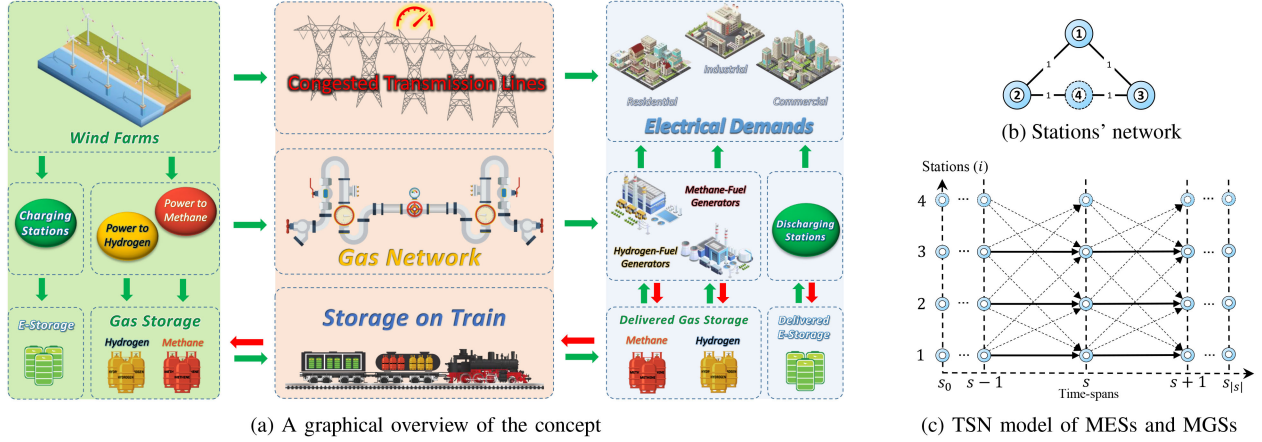


Fig. 1. The proposed integrated systems and the model of the transportation system (Some of the energy-related icons are designed by Freepik.com).

transportation system including multiple stations is presented in Fig. 1(b). The travel time between stations is specified on connecting arcs based on time spans, and each time span takes multiple hours. Also, the travel time between stations 2 and 3 takes two time spans; thereby, a virtual station 4 is considered between stations 2 and 3 to simplify the model. The arcs show the paths between stations, and the expansion of possible routes in time is presented in Fig. 1(c). The selection of travel paths for MESs and MGSs are formulated by (1) and (2). Constraint (1) implies that only one arc has to be selected between possible options in each time span. The traveling of MESs and MGSs is constrained by (2), in which the arc at time span  $ts + 1$  must be initiated from the ending node of the arc at time span  $ts$ .

The model of the swapping system for MESs and MGSs is considered based on the following assumptions. (i) Due to the nonanticipativity constraint, the traveling paths of the MESs and MGSs must be unique, and it is considered independent of scenarios; (ii) Different types of storage facilities can be swapped independently; However, the same travel paths within the same time frames can be realized simultaneously with the same train; (iii) The storage devices can start from a different location from the starting stations of trains; (iv) A delay time, defined as  $DS(i)$ , is considered by (3) for the first travel according to the arriving time of trains from the starting station; (v) The limited number of containers of MESs and cargoes of LH2/LNG tanks are considered for the sake of simplicity, but each system may contain several storage devices.

$$\sum_{i,j} A_{i,j} u_{i,j}^{(k/\bar{k}),ts} = 1 \quad (1)$$

$$\sum_j A_{j,i} u_{j,i}^{(k/\bar{k}),ts} = \sum_{j'} A_{i,j'} u_{i,j'}^{(k/\bar{k}),ts+1} \quad (2)$$

$$u_{i,j}^{(k/\bar{k}),ts} = 0 \quad ; \forall i \neq j, ts < DS(i) + 1 \quad (3)$$

### C. The MVES Elements

The description of MVES is presented in this subsection.

1) *Model of P2G*: This paper considers multiple outputs, including hydrogen and methane gases, for the P2G equipment.

P2Gs convert the electrical power into hydrogen through water electrolysis ( $2H_2O \rightarrow 2H_2 + O_2$  [41]) that can be used directly as an energy vector or further converted into methane through the methanation process ( $CO_2 + 4H_2 \leftrightarrow CH_4 + 2H_2O$  [42]). Here, methane and hydrogen gases are considered the products of P2G units, while the efficiency of methane production contains a double conversion process. Equations (4) and (5) calculate amounts of hydrogen and methane gases generated by P2G units. As reflected by (6), the power consumption of P2G equipment is limited by an upper bound, which implies that P2Gs can produce either hydrogen or methane according to the efficiencies and operational constraints.

$$G_{x,t,s}^{P2G,H_2} = Z_1^{H_2} p_{x,t,s}^{P2G,H_2} \eta_{x,t,s}^{P2G,H_2} \quad (4)$$

$$G_{x,t,s}^{P2G,CH_4} = Z_1^{CH_4} p_{x,t,s}^{P2G,CH_4} \eta_{x,t,s}^{P2G,CH_4} \quad (5)$$

$$0 \leq \left( p_{x,t,s}^{P2G,H_2} + p_{x,t,s}^{P2G,CH_4} \right) \leq P_x^{P2G,max} \quad (6)$$

2) *Model of MES*: The MES system stores and transfers the electrical energy to bypass electrical network constraints, and the model is described by (7)–(12).

$$p_{k,i,t,s}^{MES,Ch} \leq p_{k,Ch}^{MES,max} \tilde{u}_{k,t,i}^{MES,Ch} \quad (7)$$

$$p_{k,i,t,s}^{MES,Dis} \leq p_{k,Dis}^{MES,max} \tilde{u}_{k,t,i}^{MES,Dis} \quad (8)$$

$$\tilde{u}_{k,t,i}^{MES,Ch} + \tilde{u}_{k,t,i}^{MES,Dis} \leq u_{i,i}^{k,T(t)} \quad (9)$$

$$e_{k,t,s}^{MES} = e_{k,t-1,s}^{MES} + \Delta t \sum_i \left( p_{k,i,t,s}^{MES,Ch} \eta_{k,Ch}^{MES} - p_{k,i,t,s}^{MES,Dis} / \eta_{k,Dis}^{MES} \right) \quad (10)$$

$$E_k^{MES,min} \leq e_{k,t,s}^{MES} \leq E_k^{MES,max} \quad (11)$$

$$e_{k,t_0,s}^{MES} = e_{k,t_{24},s}^{MES} \quad (12)$$

Constraints (7) and (8) limit the charging and discharging of MESs, and binary variables  $\tilde{u}_{k,t,i}^{MES,Ch/Dis}$  indicate the activated operating modes of the storage at the corresponding railway stations. Constraint (9) determines the binary status

of charging/discharging of MESs for the selected railway stations (defined as  $u_{i,i}^{k,T(t)}$ ) at time span  $ts = T(t)$ . Variables  $p_{k,i,t,s}^{MES,Ch/Dis}$  reflect charging and discharging of MESs at station  $i$  and scenario  $s$ . The value of stored electrical energy at each time step  $t$  is obtained by (10) considering charging and discharging efficiencies, and (11) incorporates the limits of stored energy for MESs. The daily energy balance of MESs is reflected by (12).

3) *Model of MGS*: The MGSs for LH2/LNG tanks provide a considerable storage capacity, and the produced gases can be used for supplying remote G2Ps. The proposed model of MGSs is described by (13)–(19), which a similar model to MESs is used to reflect the model of trips for LH2/LNG tanks.

$$G_{\bar{k},i,t,s}^{MGS,Ch} \leq G_{\bar{k},Ch}^{MGS,max} \tilde{u}_{\bar{k},t,i}^{MGS,Ch} \quad (13)$$

$$G_{\bar{k},i,t,s}^{MGS,Dis} \leq G_{\bar{k},Dis}^{MGS,max} \tilde{u}_{\bar{k},t,i}^{MGS,Dis} \quad (14)$$

$$\tilde{u}_{\bar{k},t,i}^{MGS,Ch} + \tilde{u}_{\bar{k},t,i}^{MGS,Dis} \leq u_{i,i}^{\bar{k},T(t)} \quad (15)$$

$$GE_{\bar{k},t,s}^{MGS} = GE_{\bar{k},t-1,s}^{MGS} + \Delta t \sum_i \left( G_{\bar{k},i,t,s}^{MGS,Ch} \eta_{\bar{k},Ch}^{MGS} - G_{\bar{k},i,t,s}^{MGS,Dis} / \eta_{\bar{k},Dis}^{MGS} \right) \quad (16)$$

$$GE_{\bar{k}}^{MGS,min} \leq GE_{\bar{k},t,s}^{MGS} \leq GE_{\bar{k}}^{MGS,max} \quad (17)$$

$$\sum_{i \in \bar{\vartheta}} \sum_{\bar{k}} \left( G_{\bar{k},i,t,s}^{MGS,Ch,CH_4} \right) \leq \sum_{x \in \chi} G_{x,t,s}^{P2G,CH_4} \quad (18)$$

$$\sum_{i \in \bar{\vartheta}} \sum_{\bar{k}} \left( G_{\bar{k},i,t,s}^{MGS,Ch,H_2} \right) \leq \sum_{x \in \bar{\chi}} G_{x,t,s}^{P2G,H_2} \quad (19)$$

The charging and discharging of MGSs at the station  $u_{i,i}^{\bar{k},T(t)}$  and time span  $ts = T(t)$  are limited by (13) and (14), in which the variables “ $G_{\bar{k},i,t,s}^{MGS,Ch/Dis}$ ” reflect the charging and discharging values within scenario  $s$ . Constraint (15) indicates the charging/discharging modes for MGSs based on selected stations. Constraint (16) updates the hourly gas reservoir for each scenario based on charging and discharging and corresponding efficiencies, and (17) checks the reservoir boundaries for MGSs. Constraints (18) and (19) limit the value of charging LH2 and LNG tanks with methane and hydrogen for MGSs to the produced gas by the P2Gs located at the corresponding stations. Since gas storage can last longer than electricity storage, the daily energy balance is not considered for the MGSs.

### III. MULTI-VECTOR ENERGY OPERATIONAL PLANNING COORDINATED WITH CONSTRAINT MANAGEMENT

This paper uses multi-energy carriers as bridging components for the coordinated scheduling of gas and electricity networks in the presence of uncertainties to enhance the efficiency by reducing the CP to wind farms in constraint management and moving toward a zero-carbon energy supply. The proposed formulation, developed based on a stochastic mixed-integer second-order cone programming (MISOCP) model, is discussed in this section. It should be noted the method of scenario generation used in this paper is described in [43]. Besides, this study considers

the base case scenario to ensure the calculation of a specific schedule for the system operation due to the nonanticipativity constraint. In this way, the index of  $s$  contains the base case scenario as  $s_0$ , and  $s \geq 1$  is related to scenarios of uncertainties.

#### A. Model of Electrical Energy System

The operational cost of the electrical section, reflected by (20), calculates the production cost of regular generators (non-gas-fired power plants) and the cost of the startup, shutdown, and fixed cost of all generators at hour  $t$  and scenario  $s$ . The production cost of gas-fired generators (G2P elements) is considered by the objective function of the gas network. Constraints of the electrical section are presented by (21)–(29).

$$of_{t,s}^{EN} = \sum_{i \notin \beta} f(p_{g,t}^s, I_g^t, st_g^t, sd_g^t) + \sum_{i \in \beta} f(I_g^t, st_g^t, sd_g^t) \quad (20)$$

$$st_g^t - sd_g^t = I_g^t - I_g^{(t-1)} \quad (21)$$

$$st_g^t \leq I_g^\tau \quad \forall t \leq \tau \leq t + T_{on}^{min} - 1 \quad (22)$$

$$sd_g^t \leq 1 - I_g^\tau \quad \forall t \leq \tau \leq t + T_{off}^{min} - 1 \quad (23)$$

$$P_g^{min} I_g^t \leq p_{g,t}^s \leq P_g^{max} I_g^t \quad (24)$$

$$p_{g,t}^{s_0} - p_{g,(t-1)}^{s_0} \leq Ru_g I_g^{(t-1)} + RS_g st_g^t \quad (25)$$

$$p_{g,(t-1)}^{s_0} - p_{g,t}^{s_0} \leq Rd_g I_g^{(t-1)} + RD_g sd_g^t \quad (26)$$

$$p_{w,t}^s = P_{w,t,s}^{max} - p_{w,t}^s \geq 0 \quad (27)$$

Constraints (21)–(23) consider the minimum online and offline duration for electrical power generators. The generation boundary limits of generators are reflected by (24), and ramp rate limits, including the starting and shutting-down situations, are considered for the base case scenario presented by (25) and (26). The wind power dispatch is limited to the maximum generation (contracted values) as reflected by (27). Also, the wind power curtailment (per scenario) is calculated by (27), accordingly.

This paper uses the DC power flow formulation for the transmission grid as presented by (28), in which the incidence matrix of  $B_b^l$  is 1 if bus  $b$  is sending bus of line  $l$  and -1 if it is receiving bus of line  $l$ . The balance of the active power is reflected by (29) for all electrical buses. As can be seen, the power consumption of P2Gs “ $p_{x,t,s}^{P2G}$ ” is recognized as a load for the electrical grid. It should be noted that  $p_{g,t}^s$  contains the power generation of non-gas-fired generators, methane-fired generators, and hydrogen-burning turbines.

$$-PF_l^{max} \leq p_{l,t}^s = S \sum_b (B_b^l \delta_{b,t}^s / X(l)) \leq PF_l^{max} \quad (28)$$

$$\begin{aligned} \sum_{g \in \kappa} p_{g,t}^s + \sum_{w \in \Upsilon} p_{w,t}^s + \sum_{i \in \psi, k} \left( p_{k,i,t,s}^{MES,Dis} - p_{k,i,t,s}^{MES,Ch} \right) \\ = PD_{b,t}^s + \sum_{x \in \phi} p_{x,t,s}^{P2G} + \sum_l B_b^l p_{l,t}^s \end{aligned} \quad (29)$$

#### B. Model of Gas Energy System

The operational cost regarding the gas network, presented by (30), includes the value of gas purchase contracts from gas

wells, in which the cost of supplying fixed gas demands is subtracted from the objective function. The amounts of consumed gases by G2Ps are calculated by (31) and (32), in which  $Z_2$  and  $\eta_g^{CH_4/H_2}$  are the energy conversion coefficient from  $KCF$  to  $MW$  and the efficiency of G2Ps, respectively. The limits of the natural gas supply from gas wells are considered by (33).

$$of_{t,s}^{GN} = \sum_y \rho^{GN} G_{y,t,s}^{Sup} - \sum_m \rho^{GN} GD_{m,t}^{Fxd} \quad (30)$$

$$p_{g,t,s}^{CH_4} = Z_2 G_{g,t,s}^{CH_4} \eta_g^{CH_4} \quad \forall g \in \beta \quad (31)$$

$$p_{g,t,s}^{H_2} = Z_2 G_{g,t,s}^{H_2} \eta_g^{H_2} \quad \forall g \in \tilde{\beta} \quad (32)$$

$$G_y^{Sup,\min} \leq G_{y,t,s}^{Sup} \leq G_y^{Sup,\max} \quad (33)$$

Unlike electricity, it takes time to deliver gas from production resources to the demand center. In this regard, the transient model can better reflect the behavior of the gas network. However, due to the high complexity of the transient model, this paper employs the steady-state model of the high-pressure natural gas network, and the gas flow of pipelines is calculated by (34). In this equation,  $C_p$  is the pipeline constant obtained based on the gas composition and pipelines' features, and  $\pi_m^{t,s}$  is the gas pressure of node  $m$  at time step  $t$  and scenario  $s$ . The function of  $Sgn$  describes the gas flow direction in pipelines and is defined by (35). The flow direction is calculated according to the values of  $\pi_{F(p)}^{t,s}$  and  $\pi_{R(p)}^{t,s}$ , which are the gas pressure of inlet and outlet nodes. The gas flow direction is from the higher pressure to the lower pressure node.

$$GF_{p,t}^s = C_p Sgn(\pi_{F(p)}^{t,s}, \pi_{R(p)}^{t,s}) \sqrt{|\pi_{F(p)}^{t,s}|^2 - |\pi_{R(p)}^{t,s}|^2} \quad (34)$$

$$\begin{aligned} & \times Sgn(\pi_{F(p)}^{t,s}, \pi_{R(p)}^{t,s}) \\ & = \begin{cases} 1, & \pi_{F(p)}^{t,s} \geq \pi_{R(p)}^{t,s} \\ -1, & \pi_{F(p)}^{t,s} < \pi_{R(p)}^{t,s} \end{cases} \quad (35) \end{aligned}$$

The gas pressure of inlet and outlet nodes is limited by (36) and (37). If the range of gas pressure in outlet nodes was higher than the inlet node, the gas flows in the opposite direction.

$$\pi_{F(p)}^{\min} \leq \pi_{F(p)}^{t,s} \leq \pi_{F(p)}^{\max} \quad (36)$$

$$\pi_{R(p)}^{\min} \leq \pi_{R(p)}^{t,s} \leq \pi_{R(p)}^{\max} \quad (37)$$

The constraint (34) is a nonlinear equation and make the model complex; hence, by squaring both sides the function of  $Sgn$  is relaxed as follows:

$$(GF_{p,t}^s)^2 = (C_p)^2 (|\pi_{F(p)}^{t,s}|^2 - |\pi_{R(p)}^{t,s}|^2) \quad (38)$$

The  $\Gamma_1^{p,t,s}$  and  $\Gamma_2^{p,t,s}$  are defined as the square of nodal gas pressure such that the value of  $\Gamma_1^{p,t,s}$  is always greater than  $\Gamma_2^{p,t,s}$ . So, the constraint (38) becomes:

$$(GF_{p,t}^s)^2 = (C_p)^2 (\Gamma_1^{p,t,s} - \Gamma_2^{p,t,s}) \quad (39)$$

By defining  $\lambda_{p,t}^s = \Gamma_1^{p,t,s} - \Gamma_2^{p,t,s}$  and  $G_{p,t}^s > 0$  (auxiliary variable for calculating the  $|GF_{p,t}^s|$ ), (39) is transformed into a second-order cone constraint as presented by (40). Constraint (41) checks the maximum and minimum flow limits for

the pipelines based on the corresponding nodal gas pressures.

$$\lambda_{p,t}^s \geq (G_{p,t}^s / C_p)^2 \quad (40)$$

$$G_p^{\min} \leq G_{p,t}^s \leq G_p^{\max} \quad (41)$$

As it is illustrated in [40], the transformation of (39) into (40) may lead to a relaxation gap, which two methods are suggested to remove it. The one based on the sequential process is not appropriate for the comprehensive model of this paper. This paper selects the second method (also applied by [44]), which considers a slight penalty for  $\lambda_{p,t}^s$  in the objective function. The tightness of the proposed formulation will be examined in simulation results using a similar method to [40]. To ensure the square gas pressure of  $\Gamma_1^{p,t,s}$  is always greater than  $\Gamma_2^{p,t,s}$ , the nodal gas pressure limits of (36) and (37) are transformed into two sets of constraints. Constrains (42) and (43) are defined for the  $\pi_{F(p)}^{t,s}$  greater than  $\pi_{R(p)}^{t,s}$ . Also, (44) and (45) are considered for the  $\pi_{R(p)}^{t,s}$  greater than  $\pi_{F(p)}^{t,s}$ ; thereby, the natural gas flows in the opposite direction.

$$(\pi_{F(p)}^{\min})^2 - h_{p,t,s}^- M_1 \leq \Gamma_1^{p,t,s} \leq (\pi_{F(p)}^{\max})^2 + h_{p,t,s}^- M_1 \quad (42)$$

$$(\pi_{R(p)}^{\min})^2 - h_{p,t,s}^- M_1 \leq \Gamma_2^{p,t,s} \leq (\pi_{R(p)}^{\max})^2 + h_{p,t,s}^- M_1 \quad (43)$$

$$(\pi_{R(p)}^{\min})^2 - h_{p,t,s}^+ M_1 \leq \Gamma_1^{p,t,s} \leq (\pi_{R(p)}^{\max})^2 + h_{p,t,s}^+ M_1 \quad (44)$$

$$(\pi_{R(p)}^{\min})^2 - h_{p,t,s}^+ M_1 \leq \Gamma_2^{p,t,s} \leq (\pi_{R(p)}^{\max})^2 + h_{p,t,s}^+ M_1 \quad (45)$$

The constraint (46) and binary variables  $h_{p,t,s}^+$  and  $h_{p,t,s}^-$  ensure only one flow direction is possible in pipelines at each hour. The function of  $Sgn$  is redefined using a linearized description presented by (47)–(53). Constraint (47) obtains the free variable of the gas flow using the calculated values either in positive or negative directions. Constraints (48)–(50) identify the positive direction, and (51)–(53) the negative direction of gas flow.

$$h_{p,t,s}^+ + h_{p,t,s}^- \leq 1 \quad (46)$$

$$GF_{p,t}^s = GF_{p,t,s}^+ - GF_{p,t,s}^- \quad (47)$$

$$GF_{p,t,s}^+ \leq h_{p,t,s}^+ M_2 \quad (48)$$

$$GF_{p,t,s}^+ \leq G_{p,t}^s \quad (49)$$

$$GF_{p,t,s}^+ \geq G_{p,t}^s - (1 - h_{p,t,s}^+) M_2 \quad (50)$$

$$GF_{p,t,s}^- \leq h_{p,t,s}^- M_2 \quad (51)$$

$$GF_{p,t,s}^- \leq G_{p,t}^s \quad (52)$$

$$GF_{p,t,s}^- \geq G_{p,t}^s - (1 - h_{p,t,s}^-) M_2 \quad (53)$$

In this study a simplified model of compressor stations (with fixed ratio similar to transformers [29]) is considered by (54) and (55). The relationship between pressures of inlet and outlet nodes of compressors ( $0 < CR_c^{Cmp} < 1$ ) are determined by (55).

$$GF_{p,t}^s \geq 0 ; \quad \forall p \in \aleph(c) \quad (54)$$

$$\pi_{R(p)}^{t,s} \geq \pi_{F(p)}^{t,s} CR_c^{Cmp} ; \quad \forall p \in \aleph(c) \quad (55)$$

This paper does not consider the direct injection of hydrogen into the existing natural gas network due to the issues related to the safety and low compressibility of hydrogen. In contrast, the specific users of hydrogen gas are supplied by MGSs carrying

the LH2 tanks. Consequently, separate balance equations are considered for natural gas and hydrogen. The balance of natural gas generation and consumption is presented by (56), in which the injection and withdrawal of gas must be equal for all nodes, including the nodes connected to methane-fired generators and MGS stations. It should be noted, the lower speed of gas through pipelines and the possibility of changing nodal gas pressure over time make the gas balance of (56) a mandatory constraint. However, based on time steps in the day-ahead scheduling, it is assumed the gas balance constraint is established in the steady-state on an hourly basis. The gas flows of pipelines and compressors are reflected by  $GF_{p,t}^s$ . The balance of hydrogen generation and consumption is reflected by (57). In that equation,  $\Lambda$  contains all railway stations connected to node  $m$  except the stations of hydrogen-burning generators, and  $\tilde{\Lambda}$  includes stations with P2Gs or hydrogen-burning connected to node  $m$ . Sets  $\Xi$  and  $\tilde{\Xi}$  represent methane-fired and hydrogen-burning generators connected to node  $m$ , respectively. Also, sets  $\Phi$  and  $\tilde{\Phi}$  indicate MGSs contain LNG and LH2, respectively. This paper assumes that the only source of hydrogen is P2Gs, which the generated gas can be transported and used by the remote hydrogen-burning generators.

$$\begin{aligned} & \sum_{y \in \sigma} G_{y,t,s}^{Sup} + \sum_{x \in \Theta} G_{x,t,s}^{P2G,CH_4} + \sum_{i \in \Lambda} \sum_{\tilde{k} \in \tilde{\Phi}} \left( G_{\tilde{k},i,t,s}^{MGS,Dis} - G_{\tilde{k},i,t,s}^{MGS,Ch} \right) \\ & = GD_{m,t}^{Fxd} + \sum_{g \in \Xi} G_{g,t,s}^{CH_4} + \sum_p Y_p^p GF_{p,t}^s \end{aligned} \quad (56)$$

$$\sum_{x \in \Theta} G_{x,t,s}^{P2G,H_2} + \sum_{i \in \tilde{\Lambda}} \sum_{\tilde{k} \in \tilde{\Phi}} \left( G_{\tilde{k},i,t,s}^{MGS,Dis} - G_{\tilde{k},i,t,s}^{MGS,Ch} \right) = \sum_{g \in \tilde{\Xi}} G_{g,t,s}^{H_2} \quad (57)$$

### C. Coordinated Gas and Electricity Scheduling

The objective of the proposed coordinated UC problem with a stochastic formulation is presented by (58). The objective function incorporates the expected value of operational costs of electrical and gas sections, payment to swapping system, the penalty paid for CP to wind farms, and the incentive of hydrogen-burning gas generators received for clean energy generation.

$$\begin{aligned} & \min_{I, st, sd, t, s \geq 1} \sum_{p, G} \overbrace{\Omega_t^s (of_{t,s}^{EN} + of_{t,s}^{GN})}^{\text{Cost of Operation}} \\ & + \sum_{ts, k/\tilde{k}, i, j (j \neq i)} \overbrace{C_{i,j}^{k/\tilde{k}} A_{i,j} u_{i,j}^{k/\tilde{k}, ts}}^{\text{Cost of swapping system}} \\ & \sum_{w, t, s \geq 1} \underbrace{\Omega_t^s \mu^{CP} p_{w,t}^s}_{\text{CP to Wind}} - \sum_{g \in \tilde{\Xi}, t, s \geq 1} \underbrace{\Omega_t^s \mu^{H_2} p_{g,t,s}^{H_2}}_{\text{Zero-carbon Incentive}} \end{aligned} \quad (58)$$

S.t. (1) – (33) and (40) – (57)

TABLE II  
SPECIFICATIONS OF THE DIFFERENT TEST CASES

	Considered Elements		
	P2Gs	MESs	MGSs
Case-1	X	X	X
Case-2	✓	X	X
Case-3	X	✓	X
Case-4	✓	✓	X
Case-5*	✓	✓	✓

\*Proposed model of this paper.

## IV. SIMULATION RESULTS

The evaluation of the proposed model is conducted on a modified IEEE 118-bus test system connected to a 14-node gas system. The diagrams of the power, natural gas, and railway transportation sectors of the proposed test system are presented in Fig. 2. As can be seen, five wind farms are added to a geographically close area of the electrical system at buses 83, 85, 87, 89, and 92, which leads to transmission lines congestion for delivering energy to the load centers. The transmission lines connecting  $b82$  to  $b83$  and  $b92$  to buses  $b93$ ,  $b94$ ,  $b100$ , and  $b102$  are the congested tie-lines (specified by the red lines in Fig. 2(a)) that limit the delivering redundant renewable generation to other areas. Also, four P2Gs with the capacity of 500 MW power consumption and energy conversion efficiency of 75% for hydrogen and 55% for methane generation are added next to the wind farms at buses 83, 87, 89, and 92. The incorporation of every single unit of MESs or MGSs in the scheduling problem will complicate the model; hence, two containers of MESs and two cargoes of MGSs (one dedicated to LH2 and one to LNG tanks), each containing 20 units of storage facilities are considered as the elements of the MVES. It is assumed that the capacity of MESs is not enough to absorb the whole redundant wind energy. The starting station of trains is  $i19$  (at bus 19), and the waiting time for arriving the first train is one time span for all other stations. The travel time between  $i12$  and  $i92$  is two time spans, and a virtual station of  $i_V$  is considered between them to reach one time span travel time between any two stations. The penalty factor for removing the gap of second-order conic relaxation of gas flow is considered 0.0001 of gas price, which is multiplied by  $\lambda_{p,t}^s$  and added to the objective function (58). The detailed information on the proposed test system (including the data of different energy sectors) is provided in [45]. The proposed model is solved using the Gurobi solver of GAMS and on a laptop with the configuration of Intel i7 CPU 2.4 GHz and 8 GB of RAM.

This paper applies the test cases presented in Table II to evaluate the proposed model for scheduling the integrated gas and electrical networks. The basic model of Case-1 is defined without considering P2Gs, MESs, and MGSs, in which the electrical transmission capacity is insufficient to carry out the whole generation of wind farms. In Case-2, P2Gs are added to the model to participate in power delivery as a vector coupling element. Case-3 considers only MESs to investigate their impact on improving operational efficiency, and Case-4 evaluates the simultaneous application of P2Gs and MESs. The proposed model of this paper, defined as Case-5, considers all of the elements used in previous cases and MGSs as a

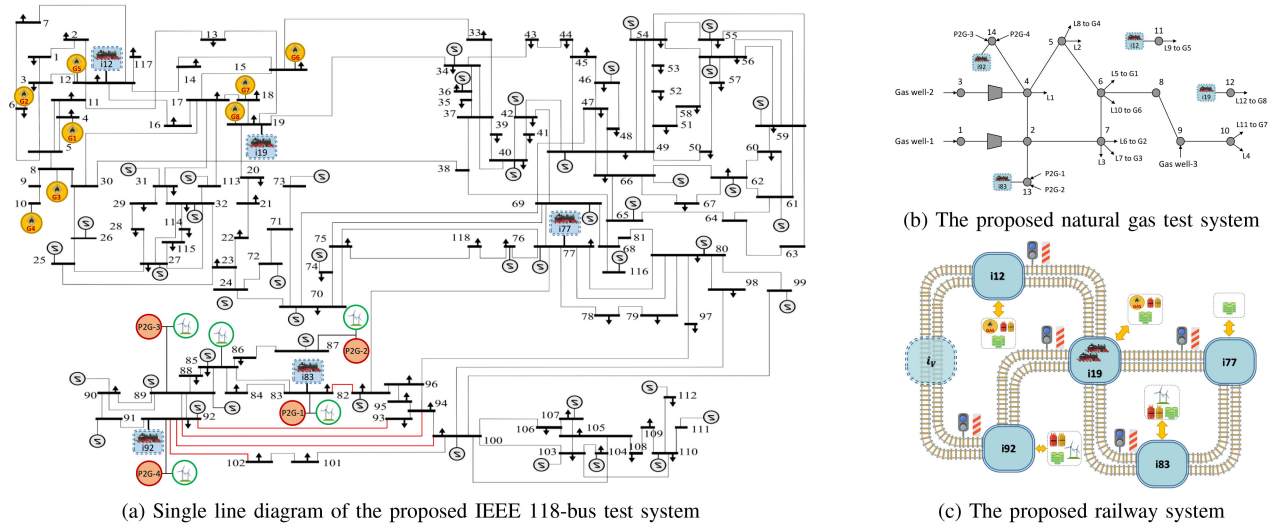


Fig. 2. The proposed integrated test system (Some of the energy-related icons are designed by Freepik.com).

TABLE III  
OPERATIONAL COSTS OF DIFFERENT TEST CASES (DETERMINISTIC CASE BASED ON THE FORECASTED VALUES)

	Electrical System				Gas System			Swapping System	Total System Operating Cost
	Production	CP	Hydrogen	Total	Gas well	P2G	Total		
Case-1	1,609,103	1,095,208	0	2,704,311	53,186	0	53,186	0	2,757,497
Case-2	1,623,161	473,761	0	2,096,922	53,506	-48,212	5,295	0	2,102,217
Case-3	1,514,792	817,901	0	2,332,693	39,370	0	39,370	640	2,372,704
Case-4	1,489,495	267,754	0	1,757,249	41,958	-41,958	0	480	1,757,729
Case-5	1,498,005	2,512	-40,950	1,459,567	66,742	-66,742	0	960	1,460,527

multi-vector energy system. This paper studies the deterministic and stochastic implementations of the proposed model to reveal the impact of both network congestion and uncertainties. In Study-A, a deterministic execution using the forecasted values for the uncertain parameters is used for comparative evaluation and sensitivity analysis. In addition, Study-B evaluates the impact of uncertainties of the variation of wind and load forecasting errors on the system operational features. The rest of this section evaluates the performance of the proposed model and compares the results obtained for the defined test cases.

#### A. Study-A

The study conducted in this section considers a deterministic execution of the model to highlight the impact of the heavily constrained networks and the uncertainties on constraint management and the energy system performance.

1) *Cost Evaluation*: The operational costs associated with the different test cases for the deterministic implementation, including the breakdown of the cost in electrical and gas sections, are compared in Table III. The cost of the electrical system consists of the production cost of generators, the CP for constraint management of wind power generators, and the revenue receives for clean energy production of hydrogen-burning generators. A considerable portion of cost increase in Case-1 imposed by CP to wind, and the rest is related to re-dispatches for electrical congestion management. Meanwhile, the generation cost and

the CP to wind farms are reduced by using the elements of the MVES. The value of CP obtained for Case-1 is \$1,095,208 which reduced over 99.8% into \$2,512 in Case-5 by employing components of the MVES. Also, the revenue for using zero-carbon generation of hydrogen-burning generators is obtained \$40,950 (2.8% of the total operational cost) for Case-5. Table III presents the cost of supplying by gas wells and the value of savings obtained by using P2Gs, separately. A large share of gas cost is reduced by using P2G units, where they use the free redundant energy of wind generation for supplying gas generators. In this regard, Case-5 obtain the highest worth of gas supply by P2Gs (\$66,742). The comparison of test cases reveals the reduction of the cost is 23.8% by utilizing P2Gs (Case-2), 13.9% by employing MESs (Case-3), 36.3% by using both P2Gs and MESs (Case-4), and finally 47% in the presence of elements of the MVES (Case-5). It should be noted 39.6% of this cost reduction is achieved by removing CP to wind, and a 7.4% decrease in operational cost is related to the enhancement of system performance in the presence of the MVES components. So, the lowest system operating cost is calculated for Case-5 (\$1,460,527) as the proposed model of this paper.

2) *Evaluation of Railway System*: Fig. 3(a) presents the hourly power of units in the electrical system for Case-5, in which non-gas generators and wind farms deploy a large amount of energy during the operation period. This figure shows that the large generation of wind farms coincides with the low-demand hours of the electrical system. So, MESs are charged during off-peak hours, and the stored energy is highly discharged during

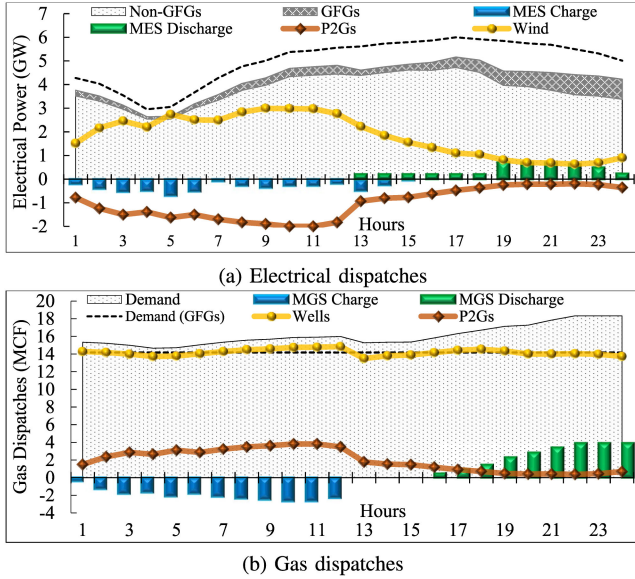


Fig. 3. Electrical and gas dispatches of different units in Case-5.

electrical peak-demand hours. In addition, P2Gs absorb the redundant wind energy, convert it to gas, and carry it out through the gas network or store it in LH2 and LNG tanks. In this regard, the production of G2Ps increases during the last hours of the operation period, when LH2 and LNG tanks reach the location of supplying G2Ps.

The hourly balance of generation and consumption for the gas system is shown in Fig. 3(b). The non-electric gas demand is assumed to be a fixed amount of 14.175 MCF during the operation period, and the curve of gas demand is obtained considering the consumption of G2Ps. It can be seen that MSGs (LH2 and LNG tanks) store a large share of P2Gs during hours of 2 to 12, which coincides with the high penetration of wind power. Also, the harvesting gas from gas wells is calculated around the value of non-electric demands of the gas system, and P2Gs are the main source of gas supply for gas-fired generators. The LNG and LH2 tanks supply methane and hydrogen for remote gas-fired generators during the last hours of operation.

The performance of considered MESs is shown in Fig. 4(a), which presents the charging and discharging, the varying locations in the electrical system, and the trips using the railway system. As can be seen, the container of MES-1 starts at *b92* and MES-2 at *b83* (labels of the transportation system are *i92* and *i83*). MES-1 is charged (absorb redundant wind energy) for two time spans and then travels to *b12* during the next two time spans. The travel between *b92* and *b12* takes two time spans and MES-1 passes through the virtual station *i<sub>v</sub>*. MES-1 discharges the stored energy during the four last timespans (12 hours). MES-2 charges for five timespans at *b83*; then, it travels during the sixth time span and reaches *b77*. After that, MES-2 discharges the whole stored energy during two timespans. It should be noted both MESs are depleted at the end of the Charge day, and the whole stored green energy of wind is used for supplying electrical demands.

Fig. 4(b) presents the obtained schedule for MSGs in charging, discharging, and traveling conditions. Both MGSs are initiated

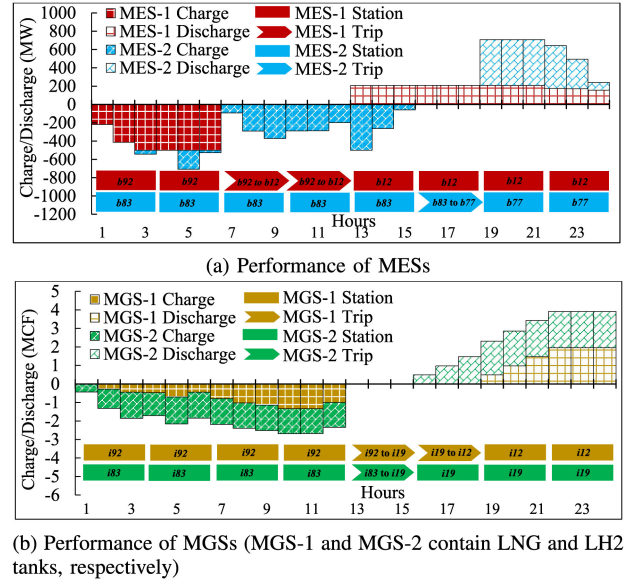


Fig. 4. Charging, discharging, and transporting of MESs and MGSs in Case-5.

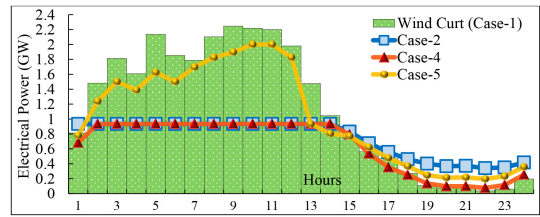


Fig. 5. Comparison of P2G energy absorption in different cases.

from stations that reside P2Gs and wind farms and absorb the redundant gas generation of P2Gs. The MGS-1 contains LNG tanks and absorbs methane generated by P2Gs located at *i92*, while MGS-2 charges LH2 tanks with hydrogen generated by P2Gs at *i83*. The MGS-1, after four time spans (nine hours) of charging, travels during the two next time spans and reaches *i12*. Then, LNG tanks supply the remote G2P located at *i12* for two time spans. For MGS-2, the absorbed hydrogen by LH2 tanks is transferred to *i19* to supply a hydrogen-burning generator. The stored hydrogen gas will be sufficient to fuel the remote hydrogen-burning generator with no access to the gas network for the last three time spans. It should be noted that LNG tanks deplete the whole stored energy, but LH2 tanks reserve an amount of 392.6 KCF hydrogen gas for the next day. The reason is that the redundant wind energy will be curtailed if not absorbed by the MGSs, and it imposes a large CP to the ESOs.

3) *Coupling Role of MVES*: The electrical absorption of P2Gs in cases 2, 4, and 5 are compared in Fig. 5. As can be seen, the pattern of wind power wastage corresponds to the changes in uptaking wind energy by P2Gs in all cases. The superiority of Case-5 can be deduced from this figure, where LNG/LH2 tanks absorb a significant portion of curtailed wind power (due to the congestion of the gas network at the moment). MGSs carry the absorbed green energy to provide gas for remote G2Ps. The

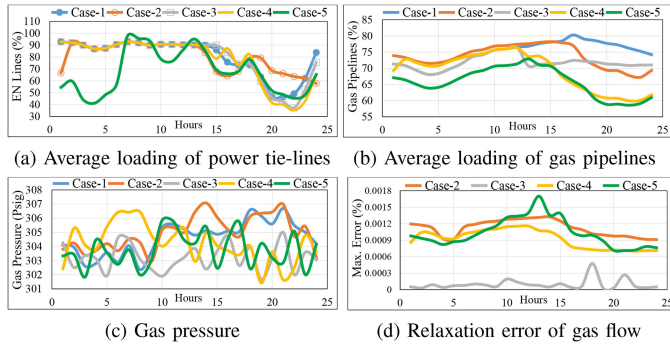


Fig. 6. Comparison of test cases from different aspects.

TABLE IV  
SOLUTION TIME OF DIFFERENT CASES (SEC)

	Case-1	Case-2	Case-3	Case-4	Case-5
Deterministic	225	351	1651	673	1786
Stochastic	820	1050	4672	2933	4799

remaining excess wind energy is absorbed by MESs and used to supply electric demands by crossing the congested power tie-lines.

Fig. 6 compares the average loading of electrical tie-lines, gas pipelines, and the average value of nodal gas pressure for different cases. The electrical tie-lines include  $l129$ ,  $l144$ ,  $l145$ ,  $l154$ , and  $l161$  that limit the delivery of green energy of wind. Fig. 6(a) shows that Case-5 (compared to the other cases) eliminates more congestion of the power tie-lines using all elements of MVES. Similarly, Fig. 6(b) compares the effect of MVES elements in reducing gas pipelines' average loading, which the best condition is evaluated for Case-5. Also, Fig. 6(c) shows the average value of nodal gas pressure is reduced in Case-5. These results are obtained for Case-5 due to the coordinated use of the gas network and transportation system as complementary energy carriers.

4) *Evaluation of the Model Performance*: The tightness of the relaxation method used for gas flow calculation is measured using the obtained values with the actual gas flow based on nodal gas pressure values. Fig. 6(d) reports the maximum hourly gap between all pipelines for different cases (the values for Case-1 is near zero). The result justifies the tightness of the proposed model. The solution time for different cases is reported in Table IV. As can be seen, the proposed MISOCP model of this paper is converged in 1786 seconds, which is a reasonable computation time for the problem. In addition, the simulation time is 4799 seconds for the stochastic implementation of the model, which is obtained using a duality gap of 0.02%.

5) *Sensitivity Evaluation*: The sensitivity evaluation of the model from different perspectives is conducted in this section. First of all, a sensitivity evaluation is performed on the swapping cost of the railway system with uniformly increasing costs between zero and \$960. The result shows that the pattern of trips is not changed since the cost of the swapping system is neglectable against the value of CP to wind. The only change

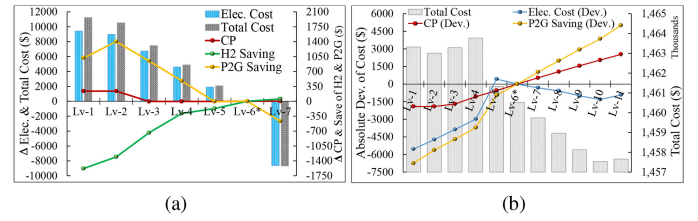


Fig. 7. Sensitivity of costs to the efficiency of (a) MESs and MGSs (b) P2Gs' energy conversion (Lv-6\* = The level with specifications of the proposed model).

is the increase in swapping cost that is directly added to the system's total cost.

Fig. 7(a) represents the sensitivity of costs to the efficiency of MESs and MGSs. Fig. 7(a) reports the absolute deviation from costs calculated for the base model of Lv-6\* (with specifications of the proposed model). Different levels of Lv-1 to Lv-6 are considered with uniformly increasing the round trip efficiency between [80% 87%] for MESs and [90% 97%] for MGSs (the efficiency of Lv-7 is 100%). As can be seen, the electricity and total costs are decreasing with increasing the efficiency of MESs and MGSs. The cost-saving related to hydrogen production is increasing due to the higher efficiency of MGSs, and the CP is decreased by increasing the efficiency of MESs and MGSs.

Fig. 7(b) performs a sensitivity of costs to the efficiency of P2Gs. Different levels (Lv-1 to Lv-11) of energy conversion efficiency are considered based on a uniform increase in the range [50% 60%] for power-to-methane and [70% 80%] for power-to-hydrogen. The absolute change in cost-saving related to P2Gs shows an increasing trend due to an increase in gas production of P2G equipment. Besides, the CP to wind increases with the enhancement of energy conversion efficiency due to a lower amount of wind power absorption. The changes in the cost of the swapping system and cost-saving related to using hydrogen are neglectable. The electricity cost increases up to the Lv-5, and then it decreases due to the greater involvement of P2Gs in gas supply. The system's total cost is decreased with increasing the efficiency except in Lv-3 and Lv-4, which is the outcome of the involved factors. The system's total cost is improved by \$5,655 for a 10% enhancement of the energy conversion efficiency.

Table VI presents a sensitivity analysis of costs to the location of railway stations, taking into consideration the relocation of the connecting points. For the first case,  $i77$  is moved to  $b89$  (the area with redundant wind energy); consequently, systems' expenditures are increased (including an additional \$35,634 of CP) due to restricted choices for destinations at the load centers. In the second case,  $i83$  is moved to  $b103$ , which yields a \$60,456 increase in CP and the system's total cost due to lower absorption of redundant wind energy. The third case considers moving stations to locations with the same conditions, and this relocation leads to a slight increase in the system's cost. In addition to the above analysis, the result shows that considering more cargoes reduces the system's expenditures but significantly increases the computational efforts.

TABLE V  
OPERATIONAL COSTS OF DIFFERENT TEST CASES IN THE PRESENCE OF UNCERTAINTY

	Electrical System				Gas System			Swapping System	Total System Operating Cost
	Production	CP	Hydrogen	Total	Gas well	P2G	Total		
Case-1	1,624,572	1,137,102	0	2,761,675	52,930	0	52,930	0	2,814,605
Case-2	1,634,436	498,578	0	2,133,013	53,124	-51,656	1,468	0	2,134,482
Case-3	1,549,041	892,166	0	2,441,207	40,732	0	40,618	640	2,482,466
Case-4	1,519,315	283,656	0	1,802,971	41,826	-42,473	-631	480	1,802,820
Case-5	1,518,419	8,646	-44,700	1,482,365	67,088	-67,330	-243	960	1,483,082

TABLE VI  
SENSITIVITY OF COSTS (\$) TO THE LOCATION OF RAILWAY STATIONS

	Changed Locations			
	[i77 to b89]	[i83 to b103]	DLSA*	Base Model
Elec. Production	1,509,538	1,598,589	1,510,082	1,498,005
CP	35,634	60,456	681	2,512
H2 Saving	-24,930	-15,944	-23,221	-40,950
P2G Saving	-61,445	-66,153	-64,854	-66,742
Transportation	1,440	1,120	1,280	960
Total Cost	1,521,682	1,644,222	1,488,822	1,460,527

\*Different locations in the area with the same conditions.

B. Study-B (Impact of Uncertainty)

The impact of uncertainties related to the prediction of wind farms’ output and the load forecasting errors on the performance of the proposed model is evaluated in this section.

1) *Cost Evaluation*: Table V presents the system’s operational costs of the stochastic implementation for different test cases. As can be seen, higher cost values are obtained by considering the uncertainties. The highest CP is calculated equal to \$1,137,102 for Case-1, which shows a 3.8% increase compared to the deterministic implementation. The value of CP to wind is raised compared to the deterministic model and reaches \$8,646 for Case-5. Besides, the reduction of CP is 99.2% for the stochastic model in Case-5. Also, the earned revenue by hydrogen-burning generators is increased by \$3,750 and reaches \$44,700 in Case-5 (3% of the system’s total cost). The gas supply of P2Gs is slightly increased in cases 2, 4, and 5, and the swapping costs in cases 3-5 are not changed compared to the results of the deterministic model. Moreover, the comparison of the total system’s cost of different test cases with Case-1 shows the reduction of the system’s total cost is 24.2% in Case-2, 11.8% in Case-3, 35.9% in Case-4, and 47.3% in Case-5. The operational cost in Case-5 is \$1,483,082 as the proposed model of this paper. It should be mentioned that 40% of the cost reduction is related to removing CP to wind farms, while the enhancement of system performance achieves a 7.3% cost reduction. In addition, the increase in the system’s total operational cost compared to the deterministic implementations is 2.1% in Case-1, 1.5% in Case-2, 4.6% in Case-3, 2.6% in Case-4, and 1.5% in Case-5. So, despite containing the lowest system’s operational cost calculated in Case-5, the lowest increase due to the inclusion of uncertainties has been obtained for this case.

2) *Performance of the MVES*: The performance of the MVES’s components is presented in Fig. 8. Based on the results, a similar traveling pattern to the deterministic case is obtained for MESs and MGSs in the presence of uncertainties. It should be noted that, due to the nonanticipativity constraint, the traveling

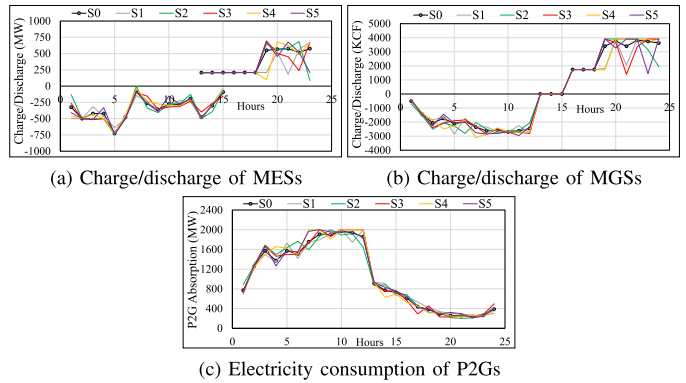


Fig. 8. Dispatches of the MES, MGS, and P2G technologies in the base case and within scenarios of uncertainties.

TABLE VII  
ELECTRICAL ENERGY DISPATCHES (MWH) WITHIN SCENARIOS AT HOUR 10 (GFG=GAS-FIRED GENERATORS/GEN.=GENERATION/CON.=CONSUMPTION)

	Scenarios					
	S0	S1	S2	S3	S4	S5
GFGs	349	329	372	357	348	340
Non-GFGs	4,337	4,186	4,450	4,362	4,333	4,338
Wind	2,982	2,996	2,910	3,046	2,990	2,734
Total Gen.	7,668	7,511	7,732	7,764	7,672	7,413
MESs	-289	-303	-273	-321	-294	-154
P2Gs	-2,000	-2,000	-1,893	-2,000	-2,000	-1,950
Demand	-5,379	-5,208	-5,565	-5,444	-5,378	-5,309
Total Con.	-7,668	-7,511	-7,732	-7,764	-7,672	-7,413

path of MESs and MGSs must be the same for all scenarios of uncertainties. However, different values of the charging or discharging of MESs and MGSs are obtained for different scenarios. As Fig. 8(a) shows, MESs charge during hours 1-15 and discharge the absorbed green energy during hours 13-24. The simultaneous MESs’ charging and discharging during hours 13 to 15 is related to different containers of MESs. According to Fig. 8(b), both MGSs charge until hour 13 and discharge between hours 16 and 24. In addition, both MESs and MGSs participate in covering uncertainties, and the values of dispatches vary within scenarios. Fig. 8(c) shows the amount of electricity absorption of P2Gs within scenarios of uncertainties, including the base case scenario.

3) *Energy Supply within Scenarios*: Table VII reflects dispatches of technologies in the generation and consumption of electrical energy at hour 10. As can be seen, the values of total generation are equal to the energy consumption of electricity demands within all scenarios, including the base case. In addition, different generation technologies dispatch different values within scenarios to meet the uncertain parameters of

TABLE VIII  
TOTAL GAS DISPATCHES OF UNITS (KCF) WITHIN SCENARIOS AT HOUR 10  
(GFG=GAS-FIRED GENERATORS/GEN.=GENERATION/CON.=CONSUMPTION)

	Scenarios					
	S0	S1	S2	S3	S4	S5
Gas Wells	14,752	14,689	14,987	14,858	14,758	14,820
P2Gs	3,815	3,815	3,611	3,815	3,815	3,720
Total Gen.	18,568	18,505	18,598	18,673	18,573	18,540
GFGs	-1,705	-1,609	-1,818	-1,744	-1,703	-1,664
MGSs	-2,688	-2,721	-2,605	-2,754	-2,694	-2,701
Demand**	-14,175	-14,175	-14,175	-14,175	-14,175	-14,175
Total Con.	-18,568	-18,505	-18,598	-18,673	-18,573	-18,540

\*\*Non-Electric Demand of Gas Network.

wind output and the hourly demand. Table VIII presents the obtained values for gas generation/consumption dispatches within scenarios of uncertainties at hour 10. As can be seen, different technologies participate in supplying gas demands, and the generation and consumption are balanced within scenarios. The results of Tables VII and VIII show that the proposed model successfully scheduled the electricity and gas for the base case and scenarios of uncertainties.

## V. CONCLUSION

A framework for multi-vector energy scheduling was proposed to facilitate the transition toward a net zero-carbon energy system. The gas network and transportation system were used as complementary energy carriers to absorb the excess green energy of renewable energy sources and bypass the electrical system congestion. Also, the railway system was used for the transportation of mobile electricity storage systems (MES) and mobile gas storage systems (MGS). The notable findings from the execution of the model are summarized as follows:

- The conducted economic evaluation in the presence of uncertainties reveals the constraint payment to wind farms was significantly reduced (over 99.2%) by applying the proposed model. Also, the hydrogen-burning generators bring a revenue equal to 3% of the total operational cost. The breakdown of the cost evaluation shows the reduction of the objective function is 24.2% by the application of power-to-gas (P2G) equipment, 11.8% by using MESSs, 35.9% by employing P2Gs plus MESSs, and 47.3% in the presence of all components together. Besides, the removal of constraint payment to wind farms has resulted in a 40% cost reduction, while the remaining 7.3% has been achieved due to improved system performance;
- The evaluation of uncertainties reveals the presence of elements of the multi-vector energy system can effectively compensate for variations and lead to the lowest increase in costs between all cases compared to the deterministic execution. In addition, the result shows that the proposed model effectively calculates the dispatches of all components within scenarios to meet demands in both electrical and gas networks;
- The railway system was successfully applied as an energy carrier, and MESSs alongside MGSs (which include liquid hydrogen or liquefied natural gas storage tanks) absorb the redundant green energy of wind and supply electricity and

gas demands. The liquid hydrogen/liquefied natural gas storage tanks supplied remote methane/hydrogen-burning generators without access to the gas network. Moreover, the coordinated operation of the gas network and transportation system relieved the congestion of electrical tie-lines and reduced gas pipelines' average loading;

- A series of sensitivity studies are performed on efficiencies and locations of railway stations. The result shows the increase of round trip efficiency of the swapping system constantly reduces the system's costs, while the higher volume of produced gases can increase the constraint payment. The sensitivity of costs to the location of railway stations shows different positions in the same area had no significant impact on the system performance, and relocation between areas can increase the system's costs.

Future research can include the capital investment costs and the constraint payment to wind as factors in the planning phase for optimization among the reinforcement of the electrical transmission network, installing more P2G equipment, or using larger LNG/LH2 tanks. Also, more accurate models representing the dynamic behavior of the gas network can be used and tested.

## REFERENCES

- [1] S. Bouckaert *et al.*, "Net zero by 2050—a roadmap for the global energy sector," *IEA*, 2021. [Online]. Available: <https://www.iea.org/reports/net-zero-by-2050>
- [2] HM Government, "The ten point plan for a green industrial revolution," 2020. [Online]. Available: [https://assets.publishing.service.gov.uk/government/uploads/system/uploads/attachment\\_data/file/936567/10\\_POINT\\_PLAN\\_BOOKLET.pdf](https://assets.publishing.service.gov.uk/government/uploads/system/uploads/attachment_data/file/936567/10_POINT_PLAN_BOOKLET.pdf)
- [3] P. Aaslid, M. Korpås, M. M. Belsnes, and O. B. Fosso, "Pricing electricity in constrained networks dominated by stochastic renewable generation and electric energy storage," *Electric Power Syst. Res.*, vol. 197, 2021, Art. no. 107169.
- [4] "Renewable Energy Foundation (REF)," *A Decade of Constraint Payments*. 2019. [Online]. Available: <https://www.ref.org.uk/ref-blog/354-a-decade-of-constraint-payments#:~:text=2019%20was%20the%20tenth%20year,discarding%208.7%20TWh%20of%20electricity>
- [5] P. Fu, D. Pudjianto, X. Zhang, and G. Strbac, "Integration of hydrogen into multi-energy systems optimisation," *Energies*, vol. 13, no. 7, 2020, Art. no. 1606.
- [6] D. F. Dominković *et al.*, "Zero carbon energy system of south east europe in 2050," *Appl. Energy*, vol. 184, pp. 1517–1528, 2016.
- [7] B. Shaffer, R. Flores, S. Samuelsen, M. Anderson, R. Mizzi, and E. Kuitunen, "Urban energy systems and the transition to zero carbon—research and case studies from the USA and europe," *Energy Procedia*, vol. 149, pp. 25–38, 2018.
- [8] Y. Li *et al.*, "Optimal stochastic operation of integrated low-carbon electric power, natural gas, and heat delivery system," *IEEE Trans. Sustain. Energy*, vol. 9, no. 1, pp. 273–283, Jan. 2018.
- [9] M. Agabalaye-Rahvar, A. Mansour-Saatloo, M. A. Mirzaei, B. Mohammadi-Ivatloo, K. Zare, and A. Anvari-Moghaddam, "Robust optimal operation strategy for a hybrid energy system based on gas-fired unit, power-to-gas facility and wind power in energy markets," *Energies*, vol. 13, no. 22, 2020, Art. no. 6131.
- [10] J. Liu, W. Sun, and G. P. Harrison, "Optimal low-carbon economic environmental dispatch of hybrid electricity-natural gas energy systems considering P2G," *Energies*, vol. 12, no. 7, 2019, Art. no. 1355.
- [11] S. Clegg and P. Mancarella, "Integrated modeling and assessment of the operational impact of power-to-gas (P2G) on electrical and gas transmission networks," *IEEE Trans. Sustain. Energy*, vol. 6, no. 4, pp. 1234–1244, Oct. 2015.
- [12] P. Zhao, C. Gu, Z. Hu, D. Xie, I. Hernando-Gil, and Y. Shen, "Distributionally robust hydrogen optimization with ensured security and multi-energy couplings," *IEEE Trans. Power Syst.*, vol. 36, no. 1, pp. 504–513, Jan. 2021.

- [13] D. Yang, Y. Xi, and G. Cai, "Day-ahead dispatch model of electro-thermal integrated energy system with power to gas function," *Appl. Sci.*, vol. 7, no. 12, pp. 1–12, 2017, Art. no. 1326.
- [14] S. Clegg and P. Mancarella, "Storing renewables in the gas network: Modelling of power-to-gas seasonal storage flexibility in low-carbon power systems," *IET Gener., Transmiss. Distrib.*, vol. 10, no. 3, pp. 566–575, 2016.
- [15] J. Liu, W. Sun, and G. P. Harrison, "The economic and environmental impact of power to hydrogen/power to methane facilities on hybrid power-natural gas energy systems," *Int. J. Hydrogen Energy*, vol. 45, no. 39, pp. 20200–20209, 2020.
- [16] H. Khani and H. E. Z. Farag, "Optimal day-ahead scheduling of power-to-gas energy storage and gas load management in wholesale electricity and gas markets," *IEEE Trans. Sustain. Energy*, vol. 9, no. 2, pp. 940–951, Apr. 2018.
- [17] G. Li, R. Zhang, T. Jiang, H. Chen, L. Bai, and X. Li, "Security-constrained Bi-level economic dispatch model for integrated natural gas and electricity systems considering wind power and power-to-gas process," *Appl. Energy*, vol. 194, pp. 696–704, 2017.
- [18] G. Pan, W. Gu, Y. Lu, H. Qiu, S. Lu, and S. Yao, "Accurate modeling of a profit-driven power to hydrogen and methane plant toward strategic bidding within multi-type markets," *IEEE Trans. Smart Grid*, vol. 12, no. 1, pp. 338–349, Jan. 2021.
- [19] Y. Li, W. Liu, M. Shahidehpour, F. Wen, K. Wang, and Y. Huang, "Optimal operation strategy for integrated natural gas generating unit and power-to-gas conversion facilities," *IEEE Trans. Sustain. Energy*, vol. 9, no. 4, pp. 1870–1879, Oct. 2018.
- [20] H. Khani, N. El-Taweel, and H. E. Farag, "Power congestion management in integrated electricity and gas distribution grids," *IEEE Syst. J.*, vol. 13, no. 2, pp. 1883–1894, Jun. 2019.
- [21] Y. Teng, Z. Wang, Y. Li, Q. Ma, Q. Hui, and S. Li, "Multi-energy storage system model based on electricity heat and hydrogen coordinated optimization for power grid flexibility," *CSEE J. Power Energy Syst.*, vol. 5, no. 2, pp. 266–274, 2019.
- [22] G. Guandalini, S. Campanari, and M. C. Romano, "Power-to-gas plants and gas turbines for improved wind energy dispatchability: Energy and economic assessment," *Appl. Energy*, vol. 147, pp. 117–130, 2015.
- [23] R. Zhang, T. Jiang, F. Li, G. Li, H. Chen, and X. Li, "Coordinated bidding strategy of wind farms and power-to-gas facilities using a cooperative game approach," *IEEE Trans. Sustain. Energy*, vol. 11, no. 4, pp. 2545–2555, Oct. 2020.
- [24] J. Liu, W. Sun, and J. Yan, "Effect of P2G on flexibility in integrated power-natural gas-heating energy systems with gas storage," *Energies*, vol. 14, no. 1, pp. 1–15, 2021, Art. no. 196.
- [25] V. Vahidinasab, M. Habibi, B. Mohammadi-Ivatloo, and P. Taylor, "Value of regional constraint management services of vector-bridging systems in a heavily constrained network," *Appl. Energy*, vol. 301, 2021, Art. no. 117421.
- [26] M. Qadrdan, H. Ameli, G. Strbac, and N. Jenkins, "Efficacy of options to address balancing challenges: Integrated gas and electricity perspectives," *Appl. Energy*, vol. 190, pp. 181–190, 2017.
- [27] T. Ding, Y. Xu, W. Wei, and L. Wu, "Energy flow optimization for integrated power-gas generation and transmission systems," *IEEE Trans. Ind. Informat.*, vol. 16, no. 3, pp. 1677–1687, Mar. 2020.
- [28] F. Qi, M. Shahidehpour, F. Wen, Z. Li, Y. He, and M. Yan, "Decentralized privacy-preserving operation of multi-area integrated electricity and natural gas systems with renewable energy resources," *IEEE Trans. Sustain. Energy*, vol. 11, no. 3, pp. 1785–1796, Jul. 2020.
- [29] C. He, L. Wu, T. Liu, and M. Shahidehpour, "Robust co-optimization scheduling of electricity and natural gas systems via ADMM," *IEEE Trans. Sustain. Energy*, vol. 8, no. 2, pp. 658–670, Apr. 2017.
- [30] Y. Sun, B. Zhang, L. Ge, D. Sidorov, J. Wang, and Z. Xu, "Day-ahead optimization schedule for gas-electric integrated energy system based on second-order cone programming," *CSEE J. Power Energy Syst.*, vol. 6, no. 1, pp. 142–151, 2020.
- [31] N. A. El-Taweel, H. Khani, and H. E. Farag, "Hydrogen storage optimal scheduling for fuel supply and capacity-based demand response program under dynamic hydrogen pricing," *IEEE Trans. Smart Grid*, vol. 10, no. 4, pp. 4531–4542, Jul. 2019.
- [32] J. Yan, F. Lai, Y. Liu, C. Y. David, W. Yi, and J. Yan, "Multi-stage transport and logistic optimization for the mobilized and distributed battery," *Energy Convers. Manage.*, vol. 196, pp. 261–276, 2019.
- [33] X. Liu, T. Zhao, S. Yao, C. B. Soh, and P. Wang, "Distributed operation management of battery swapping-charging systems," *IEEE Trans. Smart Grid*, vol. 10, no. 5, pp. 5320–5333, Sep. 2019.
- [34] M. A. Mirzaei *et al.*, "Two-stage robust-stochastic electricity market clearing considering mobile energy storage in rail transportation," *IEEE Access*, vol. 8, pp. 121780–121794, 2020.
- [35] M. Ban, J. Yu, M. Shahidehpour, D. Guo, and Y. Yao, "Electric vehicle battery swapping-charging system in power generation scheduling for managing ambient air quality and human health conditions," *IEEE Trans. Smart Grid*, vol. 10, no. 6, pp. 6812–6825, Nov. 2019.
- [36] S. Yao, P. Wang, and T. Zhao, "Transportable energy storage for more resilient distribution systems with multiple microgrids," *IEEE Trans. Smart Grid*, vol. 10, no. 3, pp. 3331–3341, May 2019.
- [37] Y. Sun, J. Zhong, Z. Li, W. Tian, and M. Shahidehpour, "Stochastic scheduling of battery-based energy storage transportation system with the penetration of wind power," *IEEE Trans. Sustain. Energy*, vol. 8, no. 1, pp. 135–144, Jan. 2017.
- [38] Y. Sun, Z. Li, M. Shahidehpour, and B. Ai, "Battery-based energy storage transportation for enhancing power system economics and security," *IEEE Trans. Smart Grid*, vol. 6, no. 5, pp. 2395–2402, Sep. 2015.
- [39] Y. Sun, Z. Li, W. Tian, and M. Shahidehpour, "A lagrangian decomposition approach to energy storage transportation scheduling in power systems," *IEEE Trans. Power Syst.*, vol. 31, no. 6, pp. 4348–4356, Nov. 2016.
- [40] Y. He *et al.*, "Decentralized optimization of multi-area electricity-natural gas flows based on cone reformulation," *IEEE Trans. Power Syst.*, vol. 33, no. 4, pp. 4531–4542, Jul. 2018.
- [41] M. Hermesmann, K. Grübel, L. Scherrotzki, and T. Müller, "Promising pathways: The geographic and energetic potential of power-to-x technologies based on regeneratively obtained hydrogen," *Renewable Sustain. Energy Rev.*, vol. 138, pp. 1–20, 2021, Art. no. 110644.
- [42] P. Balasubramanian, I. Bajaj, and M. F. Hasan, "Simulation and optimization of reforming reactors for carbon dioxide utilization using both rigorous and reduced models," *J. CO<sub>2</sub> Utilization*, vol. 23, pp. 80–104, 2018.
- [43] M. Habibi, V. Vahidinasab, and M. S. Sepasian, "A privacy-preserving approach to day-ahead TSO-DSO coordinated stochastic scheduling for energy and reserve," *IET Gener., Transmiss. Distrib.*, vol. 16, no. 1, pp. 163–180, 2022.
- [44] D. Xu, Q. Wu, B. Zhou, C. Li, L. Bai, and S. Huang, "Distributed multi-energy operation of coupled electricity, heating, and natural gas networks," *IEEE Trans. Sustain. Energy*, vol. 11, no. 4, pp. 2457–2469, Oct. 2020.
- [45] V. Vahidinasab, "MVES118bus," 2020, [Online]. Available: <http://www.vahidinasab.com/data/JNL/MVES118bus.xls>